https://doi.org/10.48048/tis.2023.6392

Monte Carlo GEANT4 Simulation Approach in Analyzing Radiation Shielding Parameter of Lombok Pumice

Rahadi Wirawan[1,*], Nurul Qomariyah[1], Teguh Ardianto[1], Dian Wijaya Kurniawidi[1], Abdul Waris[2] and Mitra Djamal[2,3]

[1]Department of Physics, FMIPA, University of Mataram, Mataram 83115, Indonesia
[2]Department of Physics, FMIPA, Bandung Institute of Technology, Bandung 40132, Indonesia
[3]Physics Study Program, Faculty of Science, Institut Teknologi Sumatera, Lampung 35365, Indonesia

([*]Corresponding author's e-mail: rwirawan@unram.ac.id)

Received: 29 August 2021, Revised: 12 December 2021, Accepted: 19 December 2021, Published: 24 November 2022

Abstract

The linear attenuation coefficient (LAC), mean free path (MFP), half-value layer (HVL), and the radiation protection efficiency (RPE) parameters of Lombok pumice powder from 3 different regions (Ijobalit, Setangi beach, and Lingsar) have been analyzed. The radiation parameter analysis was carried out to determine the pumice that potential as a raw material of radiation shielding composite. The Monte Carlo simulation using the GEANT4 toolkit was applied to analyze those parameters using a gamma-ray transmission measurement for the photon energies of ^{57}Co, ^{133}Ba, ^{54}Mn, ^{137}Cs, ^{60}Co, ^{65}Zn, ^{22}Na and ^{40}K. The GEANT4 simulation results were compared to the XCOM theoretical calculation and show that the linear attenuation coefficient parameter has a good agreement with the XCOM results based on the determination coefficient of the correlation graph (R^2 = 0.998) between those 2 approaches methods. Setangi beach pumice has a smaller LAC parameter than Ijobalit pumice and Lingsar pumice. The MFP and HVL parameter of the Setangi beach pumice indicate the absorption ability of gamma photons is low. In the low gamma energy 0.122 MeV, Ijobalit pumice and Lingsar pumice have more than 50 % RPE and are better used as a raw material of radiation shielding composite.

Keywords: Shielding, Pumice powder, Gamma-ray, GEANT4, XCOM

Introduction

The use of radiation for non-destructive material testing in the industry and radiologic application in the medical field is always equipped with an adequate protection system such as radiation shielding usage. Radiation shielding is a barrier material applied to protect equipment or the body against excessive radiation exposure from a given radiation source or undesirable radiation. Lead (Pb) is the most shielding material that effectively reduces photon radiation intensity, but it is hazardous and toxic to human health [1,2]. Nowadays, investigation of new lead-free shielding materials becomes a critical concern such as polyboron material [3], natural rock like basalt, marble, granite, and limestone [4], palladium alloy [5], glasses with different oxides [6], alternate materials in concrete [7], alloys of iron-boron [8], tungsten carbide [9], and epoxy composites [10].

The ability to absorb gamma-ray or x-ray radiation, non-toxic, abundant presence, and inexpensive are several considerations in selecting the shielding materials. Pumice is a type of natural rock produced from volcanic eruptions. Its presence is quite abundant, especially in areas that have a history of the largest volcanic eruptions such as Lombok, Indonesia. It can be used as a substitute material for cement [11], fire resistance composites [12], removal of heavy metals [13], and a fine aggregate base material for lightweight concrete [14]. Based on its elements content, pumice can potentially be used as a raw composite material of radiation shielding. Therefore it is essential to know the shielding characteristics of pumice powder as a pure material such as linear attenuation coefficient (LAC), mean free path (MFP), half-value layer (HVL) of the material, and radiation protection efficiency (RPE) parameters.

Investigation of those radiation shielding parameters can be conducted by using Numerical Monte Carlo (MC) simulation approach. The MC simulation predicts the interaction results of photon and material based on probability density functions through random number generation. This simulation is quite effective and widely employed successfully, such as in the interrogation of experimental results and

validation of bulk-material irradiation [15], wood density analysis [16], analysis of the presence and orientation of slits [17], photon absorption [18], and analyzing polymer and plastic shielding properties [19]. The numerical Monte Carlo (MC) simulation that can be employed is GEANT4. GEANT4 is an object-oriented program of interaction and particles passage through matter that have capabilities for detector and physics modeling simulation in radiation [20]. The program is used for accurate simulation in nuclear medicine and radiation protection [21].

In the present study, we investigated a LAC, MFP, HVL, and RPE of Lombok pumice for several gamma-ray energies based on the MC simulation approach using the GEANT4 toolkit. We compared it to the theoretical calculation using the XCOM cross-section program. The purpose of this study was to find Lombok pumice which has the potential as a raw material for radiation shielding composites based on those radiation parameters.

Materials and methods

Pumice samples are collected from 3 different locations, i.e. Ijobalit (East Lombok region), Setangi beach (North Lombok region), and Lingsar (West Lombok region). This study prepared pumice in powder form through a manual grinding process, as shown in **Figure 1**.

Figure 1 Lombok pumice powder samples from Ijobalit, Setangi beach, and the Lingsar region.

Determination of the radiation parameter, i.e., the linear attenuation coefficient (μ) for both Monte Carlo GEANT4 experimental simulations and XCOM, requires data of density and the constituent element composition of pumice. The density (ρ) of the pumice sample (powder form) was determined using a pycnometer based on the pumice mass and volume measured by the following formula:

$$\rho = \frac{mass}{volum} = \frac{sample\ mass}{(solvent\ mass - solvent\ mass\ trapped\ in\ sample)}\ x\ \rho_{solvent} \quad (1)$$

Acetone (C_3H_6O) with a density of 0.79 g/cm^3 is used as a solvent. **Table 1** shows the density values of pumice powder samples. The density is not significantly different from the specific gravity value [22].

Table 1 Pumice powder sample density.

Sample Number	Density (g/cm^3)		
	Ijobalit	**Setangi beach**	**Lingsar**
1	2.48587	2.21862	2.49601
2	2.48662	2.22200	2.48028
3	2.48500	2.22963	2.47015
$\rho_{average}$	2.48583 ± 0.00055	2.22342 ± 0.00414	2.48215 ± 0.00924

Meanwhile, energy dispersive x-ray spectroscopy (EDS) test was conducted to find a constituent element composition of a pumice sample. According to these sample composition and density, determination of the mass absorption coefficient $\left(\frac{\mu(E)}{\rho}\right)$ is done using XCOM 3.1 program for the photon energies of ^{57}Co (0.122 MeV; 0.1365 MeV), ^{133}Ba (0.356 MeV), ^{54}Mn (0.835 MeV), ^{137}Cs (0.662 MeV), ^{60}Co (1.173 MeV; 1.333 MeV), ^{65}Zn (1.1155 MeV), ^{22}Na (0.511 MeV; 1.275 MeV) and ^{40}K (1.461 MeV). The linear attenuation coefficient (μ) was calculated using the following formula:

$$\mu(E) = \left(\frac{\mu(E)}{\rho}\right) x \rho \tag{2}$$

and for the MFP and HVL parameters [23],

$$MFP = \frac{\int_0^\infty x e^{-\mu x} dx}{\int_0^\infty e^{-\mu x} dx} = \frac{1}{\mu} \tag{3}$$

$$HVL = \frac{\ln 2}{\mu} \tag{4}$$

The experimental simulation was carried out to investigate the gamma photon interacting with the pumice sample. The gamma-ray transmission measurement simulation (**Figure 2**) using the Monte Carlo GEANT4 9.5 program is conducted to obtain a linear attenuation coefficient to determine the others parameter. In this simulation, the dimensions of the NaI(Tl) scintillation detector used were 3 in. ×3 in. as in the previous research [17]. The density and composition of the pumice from the x-ray diffraction spectroscopy test are used to define the material composition variable in the simulation, besides its dimension. The distance between the gamma source surface and the detector surface is 15 cm. Meanwhile, pumice is placed 10 cm in front of the NaI(Tl) scintillation detector (**Figure 2(b)**). Energy spectrum simulation measurements were carried out for 10^7 beams on (history) gamma photon with the beam directed towards the pumice sample and using the Penelope interaction model. The simulation output in the histogram form of the detected energy spectrum distribution was adjusted to the experimental model and analyzed using ROOT 5.34 for the Gaussian fitting height of the peak energy spectrum detected.

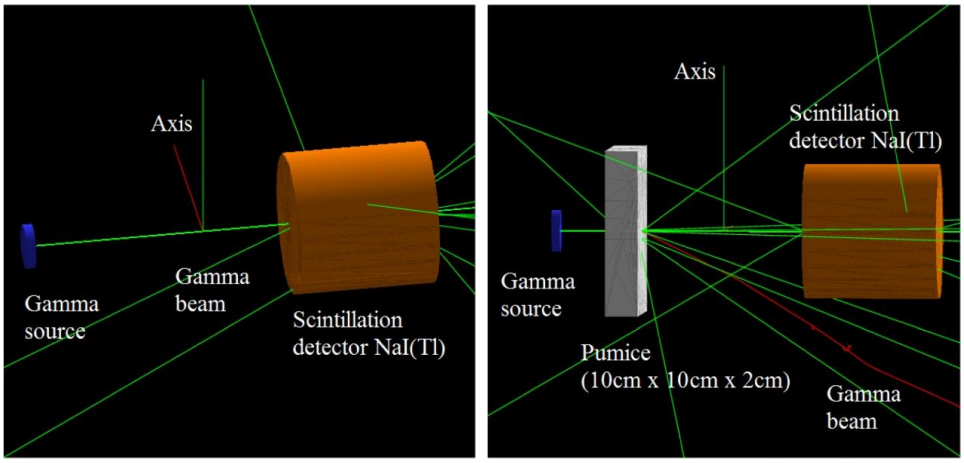

(a) (b)

Figure 2 GEANT4 simulation visualization of gamma-ray transmission; (a) The detection of gamma photon beam source by scintillation detector NaI(Tl) and (b) Detection of gamma photons that have passed through the pumice.

The linear attenuation coefficient $\mu(E)$ based on the transmission method is calculated using the Beer-Lambert formula:

$$\mu(E) = -\frac{\ln\left(\frac{I(E)}{I_s(E)}\right)}{r} \tag{5}$$

where $I(E)$ is the gamma-ray intensity that penetrates the pumice block, $I_s(E)$ is the intensity gamma-ray source detected without the presence of pumice block, and r is the thickness of pumice block [17]. The effectiveness of pumice in absorbing the photon also can be analyzed from the radiation protection efficiency (RPE) parameter by the following formula [5].

$$RPE = \left(1 - \frac{I}{I_s}\right) \times 100 \ \ \% \tag{6}$$

The intensity without and with the pumice block present is determined from the peak height results from a Gaussian fitting curve.

Results and discussion

Composition of pumice elements

Identifying the elements that make up the pumice sample can be observed through energy peaks in the graph of the X-ray diffraction spectroscopy result in **Figure 3**. As shown in the Ijobalit sample test result (**Figure 3**), the Lombok pumice sample has a higher silica element, about 26 - 32 % (**Table 2**). In **Table 2**, a large percentage of oxygen (50 - 55 %) is identified due to most elements that make up pumice which is incorporated with the oxygen element in the oxides form. The elements bound with oxygen include Al, Si, Fe, Ca, K, Na, and Mg in Al_2O_3, Fe_2O_3, SiO_2, CaO, K_2O, Na_2O and MgO.

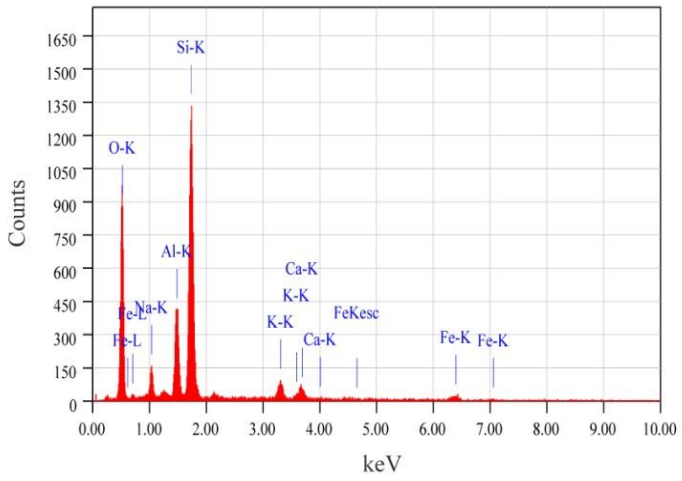

Figure 3 Diffraction spectroscopy test result of Ijobalit pumice sample.

Table 2 Elements composition of pumice from x-ray diffraction spectroscopy result.

Element	Ijobalit pumice	Setangi beach pumice	Lingsar pumice
	Percent mass (%)	Percent mass (%)	Percent mass (%)
C	-	-	2.93
O	50.59	54.16	51.26
Na	3.24	3.65	2.31
Mg	-	0.58	0.68
Al	8.7	7.02	7.71
Si	31.63	30.16	26.17
Cl	-	0.77	0.08
K	3.33	2.02	2.46
Ca	-	1.64	2.80
Fe	2.51	-	3.42
Cu	-	-	0.18

The identified elements are similar to Yaltay *et al*. [24] and Ismail *et al*. [25] research results, except for the composition of each element in the pumice sample due to differences in local geological processes of the pumice formation. As know that pumice came from volcanic eruptions, so the magma source and evolution of the crystallization process could be the reason for the difference in the elemental content and its composition [26,27]. Further studies in the geochemical review are needed for this case.

Radiation parameters of pumice

According to the X-ray diffraction spectroscopy result, we have calculated the pumice sample's mass absorption coefficient parameters using XCOM for several gamma-ray energy sources. The parameter values of those 3 different samples are presented in **Table 3**. The mass absorption coefficients decrease with the increase of the energy source. This fact can be explained based on the material parameters of interaction probability (cross-section) which are influenced by the atomic number (Z) and energy of the incident photons which are related to the dominant radiation interaction that probably occur, such as the interaction of photoelectric, Compton scattering, or pair production. The atomic numbers influence the electron density per unit mass as a significant factor affecting the mass attenuation coefficient. Furthermore, the radiation parameters are obtained using Eqs. (2) - (4), as a graph related to the photon energy as shown in **Figure 4**. The curve on the linear attenuation coefficient (LAC) graph is obtained by fitting using the 3-parameter logarithm function $y = a - b\ln(x + c)$ where a, b and c are constants. Meanwhile, the MFP and HVL curves use a quadratic polynomial fitting $y = a_0 + a_1 x + a_2 x^2$ where a_0, a_1, and a_2 are constants.

Table 3 Mass absorption coefficient (cm^2/g) pumice using XCOM.

Photon energy (MeV)	Mass absorption coefficient (cm^2/g)		
	Ijobalit	**Setangi beach**	**Lingsar**
0.122	0.14770	0.14560	0.14930
0.1365	0.14110	0.13970	0.14220
0.356	0.09906	0.09919	0.09914
0.511	0.08560	0.08576	0.08564
0.662	0.07651	0.07667	0.07654
0.835	0.06882	0.06896	0.06884
1.1155	0.05982	0.05995	0.05984
1.173	0.05832	0.05845	0.05834
1.275	0.05591	0.05603	0.05593
1.333	0.05466	0.05477	0.05467
1.461	0.05215	0.05225	0.05216

Table 4 Gaussian fitting curve height of GEANT4 simulation result.

Photon Energy (MeV)	Gaussian peak height fitting							
	No pumice		**Ijobalit pumice**		**Setangi beach pumice**		**Lingsar pumice**	
	Height	**Error**	**Height**	**Error**	**Height**	**Error**	**Height**	**Error**
0.122	1267830	622.182	617646	434.147	677866	459.843	610392	432.130
0.1365	147879	228.623	75729.4	143.48	81615.7	159.802	75091	147.406
0.356	291547	174.366	181631	137.455	190950	139.851	181726	137.325
0.511	1227810	829.973	811149	678.607	848094	693.342	812926	678.764
0.662	1456000	788.872	1009910	642.647	1049470	667.621	1009340	655.117
0.835	405865	229.616	291250	194.500	301493	197.390	291577	194.927
1.115	239504	154.643	178700	131.614	184593	134.103	178709	133.140
1.173	301418	283.029	225561	245.996	234136	253.263	227419	244.698
1.275	247797	237.126	189091	206.909	194556	209.039	189271	206.777
1.333	238796	237.387	183376	207.277	189694	204.879	183287	207.291
1.461	44453.3	95.487	34353.4	82.836	35345.9	84.972	34392.2	83.771

Table 5 RPE of pumice sample.

Photon Energy (MeV)	RPE (%)		
	Ijobalit pumice	Setangi beach pumice	Lingsar pumice
0.122	51.28	46.53	51.86
0.1365	48.79	44.81	49.22
0.356	37.70	34.50	37.67
0.511	33.94	30.93	33.79
0.662	30.64	27.92	30.68
0.835	28.24	25.72	28.16
1.115	25.37	22.93	25.38
1.173	25.17	22.32	24.55
1.275	23.69	21.49	23.62
1.333	23.21	20.56	23.25
1.461	22.72	20.49	22.63

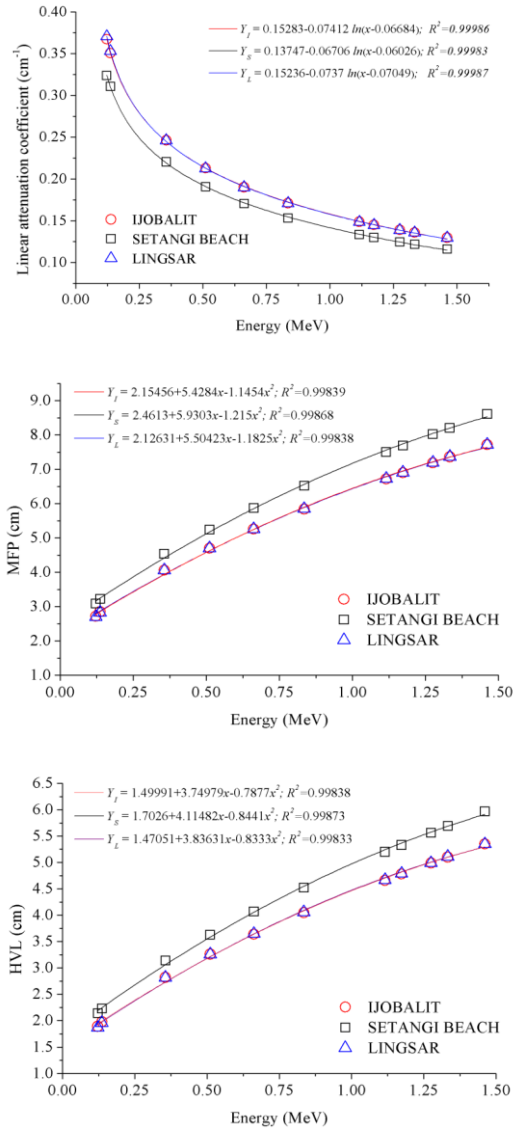

Figure 4 Radiation parameter graph based on XCOM.

According to the radiation parameter values of Lombok pumice samples (**Figure 4**), the linear attenuation coefficient, MFP, and HVL of pumice from the Ijobalit and Lingsar region have similar characteristics in the gamma photon energy analyzed. This can be observed in the constant value of the curve fitting of the data on the graph. Meanwhile, the pumice from Setangi beach has a lower linear attenuation coefficient parameter than the other 2 types of pumice. Therefore, the MFP and HVL of Setangi beach pumice are more significant than the 2 others. This value indicates that the absorption ability of gamma photons is low.

GEANT4 simulation

The simulation result of Monte Carlo GEANT4 is in the form of an energy spectrum distribution histogram. **Figure 5** shows the distribution of the energy spectrum detected NaI(Tl) scintillation detector in the transmission measurements method with the ^{60}Co source and without pumice block. It can be seen in **Figure 5(a)** that there is a decrease in the height of both peaks of detected ^{60}Co gamma-ray energy (1.173 MeV and 1.333 MeV), which through a pumice block samples (Ijobalit pumice). **Table 4** shows the peak height of each gamma photon energy curve which is detected based on the Gaussian curve fitting (**Figure (5b)**).

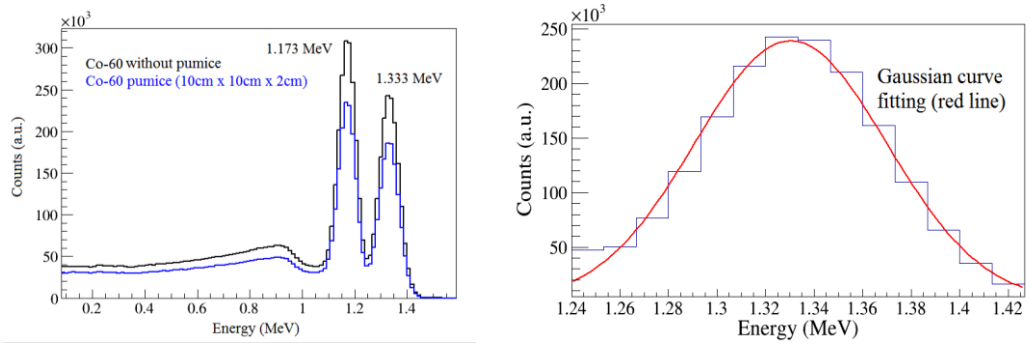

(a) (b)

Figure 5 ^{60}Co energy spectrum distribution of gamma-ray transmission measurement method and a Gaussian curve fitting peak height; (a) ^{60}Co energy spectrum distribution and (b) Gaussian curve fitting of 1.33 MeV ^{60}Co energy.

The curve characteristic of linear attenuation coefficient, MFP, and HVL was determined based on the peak height of the gamma-ray energy spectrum and using the Beer-Lambert formula Eq. (5). Using the curve fitting pattern of the 3-parameter logarithm function and the quadratic polynomial which is the same as the XCOM result, the radiation parameter curve, and associated constants are obtained as shown in **Figure 6**. The increase in the source photon energy implies a diminishing in the value of the linear attenuation coefficient. This characteristic is due to the higher probabilities of passing through material for an incoming photon with higher energy.

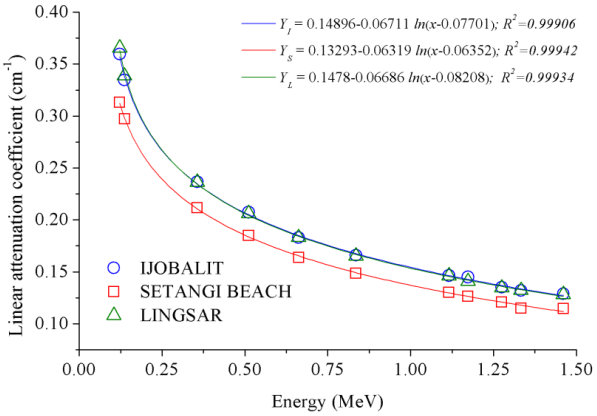

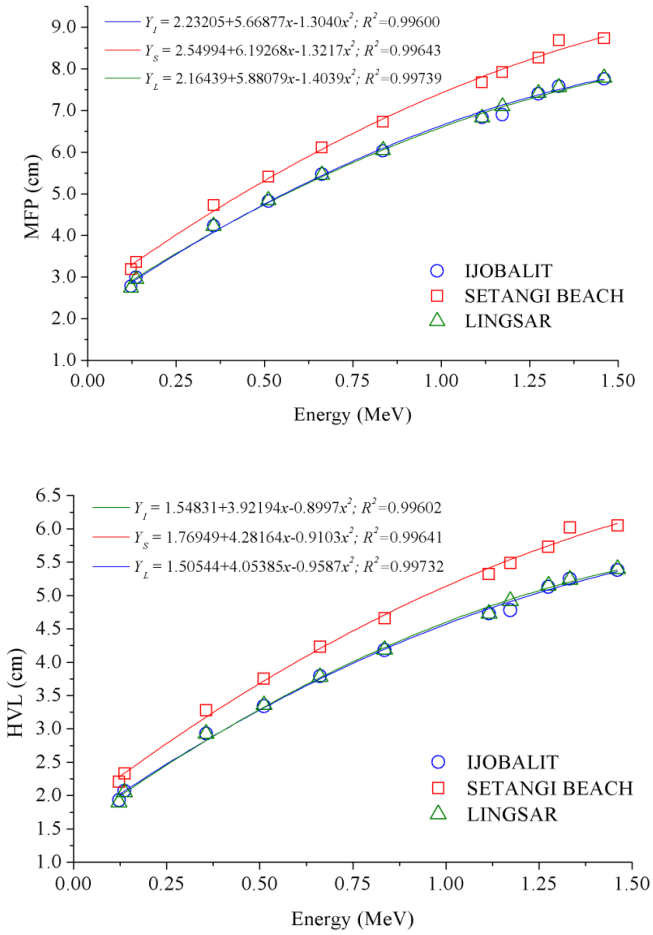

Figure 6 Radiation parameter graph based on GEANT4 simulation.

The required thickness of absorber material (shielding) to reduce the incoming gamma photon intensity can be evaluated based on the HVL value. As shown in **Figure 6**, the increase in the value of the HVL parameter linearly corresponds to the enlarging of the energy incoming gamma photon. The HVL parameter of Ijobalit pumice has a thickness almost the same as that of Lingsar pumice. The HVL value of Setangi Beach pumice is greater than the other 2 types of pumice. These results are also confirmed by the value of RPE, which is calculated using Eq. (6) and summarized in **Table 5**. At low photon energy of 0.122 MeV, the RPE of Ijobalit and Lingsar pumice were above 50 %, namely 51.28 % and 51.86 %, respectively. Meanwhile, Setangi beach pumice is 46.53 % of that energy. In the energy of 1.461 MeV, the RPE of Ijobalite and Lingsar pumice is greater than 22 %, while Setangi beach pumice is 20.49 %. Based on these results, Ijobalit pumice or Lingsar pumice has a better quality of shielding material parameters. The high value of RPE is caused by the type and amount of pumice-forming elements such as Fe and Al elements (**Table 2**). The presence of pumice constituent elements in a certain amount can make a significant contribution in reducing the intensity of gamma photons. Therefore, increasing the RPE is conducted by adding the materials containing Fe and Al elements.

Table 6 shows the linear attenuation coefficients for different gamma-ray energies using the GEANT4 simulation and the XCOM cross-section program. The linear attenuation coefficient (LAC) obtained using the Monte Carlo GEANT4 is almost similar to those of the XCOM result. This relation can be observed in the slope constant of the correlation graph $\approx$ 1.030 and 1.044 (**Figure 7**). The difference in obtaining values may occur due to the number of simulation histories and also the orientation direction setup of the gamma photon beam associated with the source type model in the simulation.

Table 6 Linear attenuation coefficient of Lombok pumice sample.

Photon energy (MeV)	Linear attenuation coefficient (μ) (cm^{-1})					
	Ijobalit		Setangi beach		Lingsar	
	GEANT4	XCOM	GEANT4	XCOM	GEANT4	XCOM
0.122	0.3596	0.3672	0.3131	0.3237	0.3655	0.3706
0.1365	0.3346	0.3507	0.2972	0.3106	0.3388	0.3530
0.356	0.2366	0.2462	0.2116	0.2205	0.2364	0.2461
0.511	0.2073	0.2128	0.1850	0.1907	0.2062	0.2126
0.662	0.1829	0.1902	0.1637	0.1705	0.1832	0.1900
0.835	0.1659	0.1711	0.1486	0.1533	0.1654	0.1709
1.1155	0.1464	0.1487	0.1302	0.1333	0.1464	0.1485
1.173	0.1450	0.1450	0.1263	0.1300	0.1409	0.1448
1.275	0.1352	0.1390	0.1209	0.1246	0.1347	0.1388
1.333	0.1320	0.1359	0.1151	0.1218	0.1323	0.1357
1.461	0.1289	0.1296	0.1146	0.1162	0.1283	0.1295

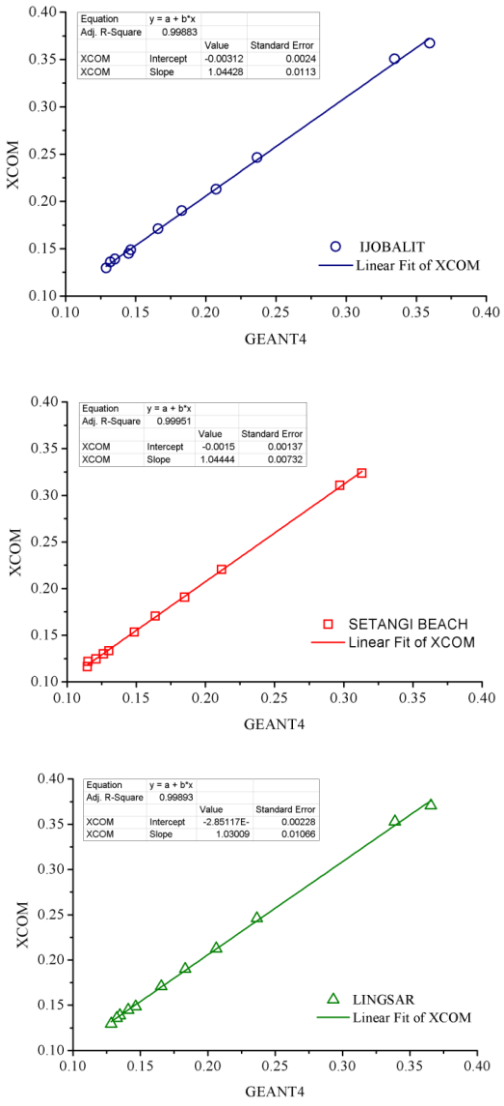

Figure 7 Graph correlation of linear attenuation coefficient between GEANT4 and XCOM.

Conclusions

Monte Carlo GEANT4 simulation approach with gamma-ray transmission method successfully applied in analyzing radiation parameters of the pumice. The value of pumice radiation parameters depends on the radiation energy and material composition. Setangi beach pumice has a smaller linear attenuation coefficient (LAC) than Ijobalit pumice and Lingsar pumice. The MFP and HVL parameter indicates that the absorption ability of gamma photons of Setangi beach pumice is low compared to the 2 other pumice. According to the RPE, Ijobalit pumice and Lingsar pumice are better used as a raw material of radiation shielding composite, especially for energy 0.122 MeV (> 50 %) or less. The determination coefficient value ($R^2 \approx 0.998$) of the linear attenuation coefficient curve indicates a match between GEANT4 and XCOM.

Acknowledgements

We are grateful to the University of Mataram for supporting this research through BLU (PNBP), Indonesia, funding.

References

[1] NJ AbuAlRoos, NAB Amin and R Zainon. Conventional and new lead-free radiation shielding materials for radiation protection in nuclear medicine: A review. *Radiat. Phys. Chem.* 2019; **165**, 108439.
[2] AL Wani, A Ara and JA Usmani. Lead toxicity: A review. *Interdiscipl. Toxicol.* 2015; **8**, 55-64.
[3] R Biswas, H Sahadath, AS Mollah and MF Huq. Calculation of gamma-ray attenuation parameters for locally developed shielding material: Polyboron. *J. Radiat. Res. Appl. Sci.* 2016; **9**, 26-34.
[4] SS Obaid, MI Sayyed, DK Gaikwad and PP Pawar. Attenuation coefficients and exposure buildup factor of some rocks for gamma ray shielding applications. *Radiat. Phys. Chem.* 2018; **148**, 86-94.
[5] O Agar, MI Sayyed, F Akman, HO Tekin and MR Kaçal. An extensive investigation on gamma ray shielding features of Pd/Ag based alloys. *Nucl. Eng. Tech.* 2019; **51**, 853-9.
[6] O Agar, MI Sayyed, HO Tekin, KM Kaky, SO Baki and I Kityk. An investigation on shielding properties of BaO, MoO_3 and P_2O_5 based glasses using MCNPX code. *Results Phys.* 2019; **12**, 629-34.
[7] G Tyagi, A Singhal, S Routroy, D Bhunia and M Lahoti. Radiation shielding concrete with alternate constituents: An approach to address multiple hazards. *J. Hazard. Mater.* 2020; **404**, 124201.
[8] A Levet, E Kavaz and Y Özdemir. An experimental study on the investigation of nuclear radiation shielding characteristics in iron-boron alloys. *J. Alloy. Comp.* 2020; **819**, 152946.
[9] NJ AbuAlRoos, MN Azman, NAB Amin and R Zainon. Tungsten-based material as promising new lead-free gamma radiation shielding material in nuclear medicine. *Phys. Med.* 2020; **78**, 48-57.
[10] MJR Aldhuhaibat, MS Amana, NJ Jubier and AA Salim. Improved gamma radiation shielding traits of epoxy composites: Evaluation of mass attenuation coefficient, effective atomic and electron number. *Radiat. Phys. Chem.* 2021; **179**, 109183.
[11] AM Zeyad, A Husain and BA Tayeh. Durability and strength characteristics of high-strength concrete incorporated with volcanic pumice powder and polypropylene fibers. *J. Mater. Res. Tech.* 2020; **9**, 806-18.
[12] H Binici and O Aksogan. Fire resistance of composite made with waste cardboard, gypsum, pumice, perlite, vermiculite and zeolite. *SN Appl. Sci.* 2019; **1**, 1244.
[13] MS Amin, FS Hashem and SMA El-Gamal. Utilization of OPC-Pumice composites for efficient heavy metals removal. *J. Taibah Univ. Sci.* 2018; **12**, 765-73.
[14] KMA Hossain. Properties of volcanic pumice based cement and lightweight concrete. *Cement Concr. Res.* 2004; **34**, 283-91.
[15] S Sharma, L Vo, MP Pfeifer, WL Dunn, WJ McNeil and AA Bahadori. Bulk material interrogation experimental results and validation with Geant4 for replacement of dangerous radiological sources in oil-well logging industries. *Appl. Radiat. Isot.* 2021; **170**, 109602.
[16] A Sharma, A Singh and BS Sandhu. A compton scattering technique for wood characteristics using FLUKA monte carlo code. *Radiat. Phys. Chem.* 2021; **182**, 109364.
[17] R Wirawan, LM Angraini, N Qomariyah, A Waris and M Djamal. Gamma backscattering analysis of flaw types and orientation based on monte carlo GEANT4 simulations. *Appl. Radiat. Isot.* 2020; **155**, 108924.
[18] X Huyan, O Naviliat-Cuncic, P Voytas, S Chandavar, M Hughes, K Minamisono and SV Paulauskas. Geant4 simulations of the absorption of photons in CsI and NaI produced by electrons with energies

up to 4 MeV and their application to precision measurements of the β-energy spectrum with a calorimetric technique. *Nucl. Instrum. Meth. Phys. Res. A Accel. Spectrometers Detectors Assoc. Equip.* 2018; **879**, 134-40.

[19] O Gurler and UA Tarim. Determination of radiation shielding properties of some polymer and plastic materials against gamma-rays. *Acta Phys. Pol.* 2016; **130**, 236-8.

[20] J Allison, K Amako, J Apostolakis, H Araujo, P Arce, M Asai, D Axen, S Banerjee, G Barrand, F Behner, L Bellagamba, JF Boudreau, L Broglia, A Brunengo, H Burkhardt, S Chauvie, J Chuma and D Zschiesche. GEANT4-a Simulation toolkit. *Nucl. Instrum. Meth. Phys. Res. A Accel. Spectrometers Detectors Assoc. Equip.* 2003; **506**, 250-303.

[21] J Allison, K Amako, J Apostolakis, H Araujo, PA Dubois, M Asai, G Barrand, R Capra, S Chauvie, R Chytracek, GAP Cirrone, G Cooperman, G Cosmo, G Cuttone, GG Daquino, M Donszelmann, M Dressel, G Folger, F Foppiano, J Generowicz, ..., H Yoshida. Geant4 Developments and Applications. *IEEE Trans. Nucl. Sci.* 2006; **53**, 270-8.

[22] A Bakis. The usability of pumice powder as a binding additive in the aspect of selected mechanical parameters for concrete road pavement. *Materials* 2019; **12**, 2743.

[23] H Akyildirim. Olivine mineral used in concrete for gamma-ray shielding. *Arabian J. Geosci.* 2019; **12**, 264.

[24] N Yaltay, CE Ekinci, T Çakır and B Oto. Photon attenuation properties of concrete produced with pumice aggregate and colemanite addition in different rates and the effect of curing age to these properties. *Progr. Nucl. Energ.* 2015; **78**, 25-35.

[25] AIM Ismail, OI El-Shafey, MHA Amr and MS El-Maghraby. Pumice characteristics and their utilization on the synthesis of mesoporous minerals and on the removal of heavy metals. *Int. Sch. Res. Not.* 2014; **2014**, 259379.

[26] Y Zhang, Z Zeng, X Yin, H Qi, S Chen, X Wang, Y Shu and Z Chen. Petrology and mineralogy of pumice from the Iheya North Knoll, Okinawa Trough: Implications for the differentiation of crystal-poor and volatile-rich melts in the magma chamber. *Geol. J.* 2018; **53**, 2732-45.

[27] Z Shikui, G Kun, Z Tong, Y Zenghui, W Shujie, C Zongwei and Z Xia. Geochemical features of trace and rare earth elements of pumice in middle Okinawa Trough and its indication of magmatic process. *J. Ocean Univ. China* 2017; **16**, 233-42.